Kinetic analysis of tritium release from irradiated biphasic lithium ceramics Li_4SiO_4-Li_2TiO_3 with different phase ratios

S. Askerbekov [a,b,*], Y. Chikhray [b], T. Kulsartov [a,b], A. Akhanov [a], A. Shaimerdenov [a], M. Aitkulov [a], Zh. Bugybay [a], I. Kenzhina [a,b], Sh. Gizatulin [a], R. Knitter [c], J. Leys [c]

[a] The Institute of Nuclear Physics, Almaty, Kazakhstan
[b] Institute of Experimental and Theoretical Physics, al-Farabi Kazakh National University, Almaty, Kazakhstan
[c] Karlsruhe Institute of Technology, Karlsruhe, Germany

Keywords:
Two-phase lithium ceramics
Tritium
Neutron irradiation
Tritium release
TDS
RGA

A B S T R A C T

This paper analyzes the kinetics of tritium release from biphasic Li_2TiO_3/Li_4SiO_4 lithium ceramics using thermal desorption spectroscopy after neutron irradiation at the WWR-K reactor. Samples with different Li_2TiO_3 contents (25 mol% and 35 mol%) in the Li_4SiO_4 main phase, fabricated by the KALOS process at the Karlsruhe Institute of Technology, were irradiated at a low temperature and a thermal neutron flux of 2×10^{13} n/(cm^2·s) during 21.5 effective full power days until accumulating a fluence of 3.7×10^{19} n/cm^2.

The experimental results confirm the significant influence of phase composition on the processes of tritium release. The analysis allowed us to develop a reasonable mechanism of tritium release during linear heating up to 1173 K.

Tritium was found to be uniformly distributed throughout the ceramic volume and its release is closely related to the microstructural characteristics of the material. Key factors affecting the process include the presence and distribution of traps and defects interacting with the external surface of the sample. The release process of these traps is determined by the transport of tritium to the boundaries, followed by desorption mainly in the form of HT molecules and has three main peaks.

Samples with 25 mol% Li_2TiO_3 showed high activation energy values, indicating the presence of more stable traps and complex tritium transport pathways. With an increased Li_2TiO_3 content of 35 mol%, a decrease in activation energy was observed, indicating a faster desorption process, probably due to changes in microstructure or the number of active defects facilitating tritium release at lower temperatures.

1. Introduction

In the global transition to sustainable and clean energy sources, fusion technology emerges as one of the most promising areas of future energy supply. However, there are many challenges on the way to the commercialization of this technology, one of which is the development and optimization of materials for the efficient production of tritium, a key component needed to sustain fusion reactions. In this context, biphasic Li_2TiO_3/Li_4SiO_4 ceramics, such as Li_4SiO_4 (LOS) with Li_2TiO_3 (LMT) additions, stand out as promising materials with a number of unique properties, including high chemical stability, high melting point, and efficiency in tritium release [1–4]. The combination of the LOS phase, which provides high lithium density, promotes efficient tritium generation, with the LMT phase that reinforces the thermal and mechanical stability of the material, seems advantageous. In the Helium Cooled Pebble Bed (HCPB) concept for the EU DEMO reactor, a mixture containing up to 35 mol% LMT in LOS is considered as a ceramic breeder material [5].

The samples studied in this work are biphasic lithium-based ceramics with phase compositions of 25 mol% LMT and 75 mol% LOS, as well as 35 mol% LMT and 65 mol% LOS. These materials were fabricated using the innovative KALOS (KArlsruhe Lithium OrthoSilicate) process developed at the Karlsruhe Institute of Technology (KIT) [6]. Previous studies revealed that these materials can maintain high tritium release efficiency even at extreme irradiation levels, making them ideal candidates for use in a future fusion power cycle [7–9].

The aim of this work was to investigate the kinetics of tritium release from neutron-irradiated LMT/LOS biphasic ceramics using thermal

* Corresponding author.
E-mail address: askerbekov@physics.kz (S. Askerbekov).

desorption spectroscopy (TDS), with special attention paid to the influence of phase ratio on tritium release processes.

As part of the study, a comprehensive work was performed to analyze the kinetics of tritium release from biphasic lithium ceramics after their irradiation at the WWR-K research reactor in Almaty (Kazakhstan). The main point of this work is the achievement of high thermal neutron fluences, of the order of 3.7×10^{19} n/cm^2, which significantly exceeds the parameters achieved in previous studies by other authors [10–14]. This allowed an extensive analysis of the effects of high levels of irradiation on the properties of these materials and their tritium release behavior.

As a result of post-reactor TDS experiments, gas release processes were analyzed to describe the mechanisms of tritium release from biphasic lithium ceramics of different phase composition. Therefore, it was possible to establish the regularities of tritium desorption processes, revealing the key characteristics of the investigated materials. Based on the analysis of thermodesorption curves, the activation energies of the main stages of tritium desorption from lithium ceramics at linear heating up to 1173 K were determined. The results of the study showed that the change of the phase ratio in biphasic lithium ceramics has a significant effect on the kinetics of tritium release.

Therefore, this study not only expands the existing theoretical basis for determining the effect of irradiation on the kinetics of tritium release from biphasic lithium ceramics, but also provides important practical recommendations for further development and optimization of the technology of production of materials for fusion reactors. The uniqueness of the studied samples and the results obtained make a significant contribution to the development of fusion technologies, bringing us closer to the creation of safe, efficient and environmentally friendly energy sources in the future.

2. Samples studied

2.1. Samples fabrication

This paper studies material samples fabricated by KIT using the KALOS process, developed as so-called advanced ceramic breeder (ACB) pebbles within the EUROfusion programme [6]. The samples are biphasic lithium-based ceramics with two different phase ratios: 25 mol % LMT + 75 mol% LOS (denoted as 25 %LMT), and 35 mol% LMT + 65 mol% LOS (denoted as 35 %LMT). These materials were studied in order to evaluate their ability to generate and accumulate tritium under conditions of neutron radiation conditions. The use of different phase ratios enables us to study the influence of composition on the characteristics of ceramics, which is of key importance for optimizing the materials for their use in fusion reactors.

The melt-based KALOS process is an innovative approach to the production of lithium ceramic materials. This method stands out due to its high production rate of 2 kg/h with a yield of over 95 %. Because of the rapid quenching of molten droplets, the pebbles exhibit a specific dendritic microstructure that results in a superior chemical and thermal stability [15]. After the production in the KALOS process, the pebbles undergo a strict quality control. Each batch is tested with regard to e.g. their chemical and phase composition, porosity, mechanical stability etc. [6]. This approach guarantees high quality ceramics that meet all technical requirements and specifications, making the KALOS process particularly valuable for applications in fusion requiring high material reliability.

2.2. Samples irradiation

Samples of lithium ceramics of different phase composition (25 % LMT + 35 %LMT) were irradiated at the WWR-K reactor under identical conditions. This provided a precise determination of the influence of different phases on the behavior of materials under the influence of neutron radiation. The samples, placed in the axial center of the reactor core, were irradiated with thermal neutrons with a flux of 2×10^{13} n/(cm^2·s). The irradiation position is in the core periphery, behind an annular beryllium reflector. The experiment was conducted for 21.5 EFPD (effective full power days) at a reactor thermal power level of 6 MW, and the temperature of the samples during irradiation did not exceed 325 K. The samples of different phase composition were wrapped in aluminum foil and then placed in specially designed sub-capsules [16]. Sub-capsules filled by argon gas to create an inert environment. Sub-capsules were installed in the standard capsule of WWR-K reactor. The capsule and sub-capsules made of low-activated aluminum alloy SAV-1. The arrangement of sub-capsules in the capsule ensured uniform irradiation and maximally equal conditions for all samples, regardless of their phase composition.

Table 1
Characteristics of lithium ceramic samples.

Batch	25 %LMT	35 %LMT
Mass, mg	300.3	301.1
Li-6, mg	4.04	3.58
Density (pebble), g/cm^3	2.464	2.612
Density (pebble bed), g/cm^3	1.52 ± 0.03	1.56 ± 0.03
Nuclear reaction rate ^{6}Li(n,α)T, reactions/(cm^3•s)	2.87E+13	2.98E+13
Amount of tritium generated in pebbles, mol/mg	1.05E 8	1.09E 8
Damage dose (estimated by NRT approach), dpa	1.4	1.5
Li-6 burnup, %	2.4	2.6

Table 2
Characteristics of selected samples: weighing, dimensions.

Sample	No.	Sample mass, mg	Pebble diameter, mm
25 %LMT	1	1.47 ± 0.02	1.26 ± 0.02
	2	1.17 ± 0.02	1.15 ± 0.05
	3	1.27 ± 0.02	1.18 ± 0.03
35 %LMT	4	1.13 ± 0.02	1.20 ± 0.01
	5	1.15 ± 0.02	1.24 ± 0.01
	6	1.20 ± 0.02	1.23 ± 0.02

2.3. Neutron-physical calculations

To predict tritium formation in the biphasic lithium ceramics, the developed model of the core of the WWR-K reactor and the capsule containing the sub-capsules with samples, as well as MCNP6.2 code with ENDF/B-VII.1 nuclear database for analyzing particle transport, were used. Theoretical calculations were based on the density and total volume of irradiated samples, as well as the nuclear reaction rate of tritium generation. Over an irradiation period of 21.5 EFPD, the amount of tritium generated in the ceramics per unit volume was estimated (see Table 1).

2.4. Characterization and weighing of samples before TDS

Three samples were selected from each batch after irradiation in the reactor for the present experiments. Before the experiment, each sample was characterized and weighed (see Table 2).

The visual appearance of the samples before the TDS experiments is presented in Fig. 1, where the cell size corresponds to approx. 1 × 1 mm. It is noticeable that the samples with a lower content of 25 %LMT phase have a darker shade compared to 35 %LMT pebbles. It should be noted here that the dark color of the samples is due to the deficit of oxygen atoms on the surface [17]. Possibly the main phase (LOS), is more susceptible to loss of oxygen atoms under reactor irradiation conditions, this may be the subject of future research.

Also, notches resulting from the production of different sizes are observed on the surface of the samples (most clearly seen in sample 5), which significantly affect the surface area of the sample, which, in turn, affects the dynamics of the tritium release process.

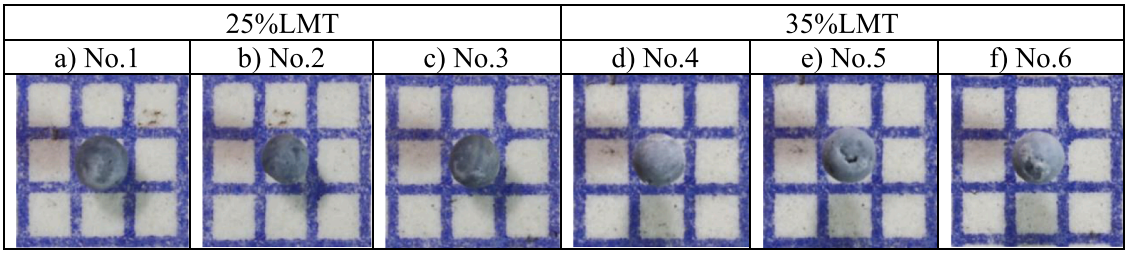

Fig. 1. Samples before TDS experiments.

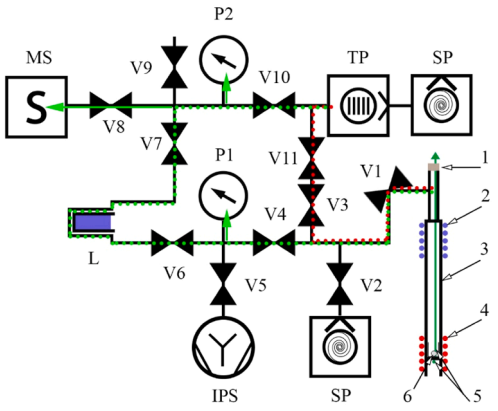

1 – hermetic connector; 2 – cooling, 3 – experimental cell; 4 – heater; 5 – thermocouples; 6 – samples; P1-P2 – pressure sensors; TP – turbomolecular pump; MS – mass-analyzer; IPS – magnetic discharge pump; SP – scroll pump; L – nitrogen trap

Fig. 2. Modernized layout of the TDS set-up, 1 – hermetic connector; 2 – cooling, 3 – experimental cell; 4 – heater; 5 – thermocouples; 6 – samples; P1-P2 – pressure sensors; TP – turbomolecular pump; MS – mass-analyzer; IPS – magnetic discharge pump; SP – scroll pump; L – nitrogen trap.

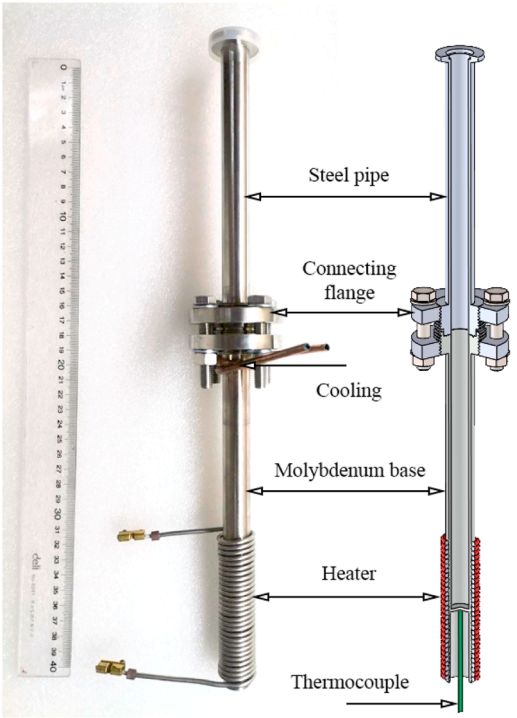

Fig. 3. Appearance and 3D model of the ED.

3. Experiments

In a previous work, it was found that generated tritium is released in the form of HT without forming heavy-water compounds [18], but the presence of significant amounts of water vapor greatly affected the TDS spectrum. Based on these data, a decision was taken to modernize the TDS unit (see. Fig. 2). A key aspect of the upgrade was the integration of a nitrogen trap and a pre-pumping path. The integration of the nitrogen trap significantly improved the vacuum conditions during experiments, increased the sensitivity of the system, and minimized the influence of aqueous components on measurements of other spectra. In addition, the research plans provide for degassing of the nitrogen trap upon completion of all experiments. It should be noted here that the analysis of residual gases confirmed the absence of heavy-water compounds, which was an additional confirmation of the accuracy of the applied experimental methodology.

The integration of the pre-pumping path (shown in red dashed line in the diagram) is aimed at minimizing the penetration of atmospheric gases into the working path (shown in green dashed line in the diagram) of the unit after opening the experimental device (ED) during sample reloading. Due to the use of a turbomolecular pump (TP), direct pumping of air through the pre-pumping path is provided, which guarantees high vacuum purity in the working path - a critical factor for achieving more accurate research results.

The idea was to connect a one-piece molybdenum working chamber to the top of the ED through a metal-on-metal "male"-"female" flange through a copper pad, and the top of the ED was molded in one piece (without welding). Appearance and geometry of the ED are shown in the Fig. 3. Thermocouples are placed as close to the samples as possible, the first thermocouple is introduced through a hermetic connector and fixed near the sample, the second one is installed directly at the level of the samples through the chamber wall, which allows to control the temperature mode in the test area with high accuracy.

In addition, cooling was provided to prevent overheating of the steel elements of the ED, maintaining the temperature not higher than 360 K above the molybdenum part of the ED. This measure prevents the increased release of various gases from the structural materials of the unit during high-temperature experiments, which has a positive effect on the purity of the experiment. All these improvements together significantly increase the efficiency of the unit, making it more adaptable to complex experiments with a single pebble within a large-volume unit.

3.1. Procedure for conducting research

The procedure for conducting research using TDS is a complex process involving several important steps:

1. Sample placement: A single test pebble, after weighing and characterization, is placed in a molybdenum crucible, which is then installed in the ED.
2. Vacuumizing the system: After sample reloading, the ED is sealed and a high vacuum to a pressure of about 10^{-3} Pa is created by pumping with a TP through the primary pumping path. The pressure

Table 3
Order of experiments by heating rate and sample batches.

Heating rate, K/min	25 %LMT	35 %LMT	Blank
5	No.1	No.4	No.7
10	No.2	No.5	No.8
20	No.3	No.6	No.9

is monitored by a TP sensor. The pumping is then switched to the operating mode and data registration begins.

3. Heating: The sample is heated linearly at rates of 5, 10 or 20 K/min to a maximum temperature of 1173 K. At this temperature, the sample is held for 5 mins to stabilize the processes in the sample.
4. Cooling: After the heating stage is completed, the sample is cooled naturally to room temperature.
5. Temperature control: The temperature during the experiment is controlled using a PID (Proportional–integral–derivative) controller. An external thermocouple is used to monitor the temperature.
6. Registration of changes in the gas compositions: The mass spectrometer continuously analyzes the composition of the gas (M1-M46) released from the sample during the heating process, which allows to follow the dynamics of desorption of different components.
7. Additional records: In addition to the gas analysis, temperature and absolute pressure changes are recorded using two thermocouples T1-T2 and pressure sensors P1-P2, which provide additional information on the real-time status of the unit parameters.
8. *Re*-weighing and characterization: After the tests are completed, each sample is re-weighed and undergoes additional characterization to assess the changes that occurred as a result of the TDS experiments.

The order of experiments by heating rate and batches of samples is presented in the Table 3, where sample numbers coincide with the sequence of experiments, and the designation “blank” represents experiments without a sample, but an empty crucible.

4. Results and discussion

During TDS, comprehensive mass spectrometer data were obtained, as well as values of absolute pressures in the sample chamber (P1) and in the mass spectrometer chamber (P2), supplemented by sample temperatures. All these data were carefully processed, allowing the partial pressure of the gases present in the mass spectrometer chamber to be estimated. Detailed decoded mass spectra for the temperature range from 400 to 1200 K, which is the most informative part of the experiments, are presented below (see. Fig. 4).

The pressure in the sample chamber (P1) is higher due to its location in the pumping scheme, before the nitrogen trap relative to the TP, which indicates the presence of water vapor. At the same time, the pressure in the mass spectrometer chamber (P2) accurately reflects the total content of all gases recorded by mass-analyzer. Comparison of the data obtained with control values from the blank experiment shows that the spectra of most of the atmospheric gas species remain unchanged. However, differences are observed for carbon-containing species such as CO and CO_2. Possible mechanisms of formation of these gas species have been discussed in detail by the authors in a previous publication [18]. In the present experiments, despite a significant improvement in the vacuum conditions of the working chamber, the data of blank experiments indicate the presence of gas species such as H_2, CO, CO_2, and other atmospheric components in the ED chamber, which significantly affects the processes of tritium release. The effect of the presence of hydrogen

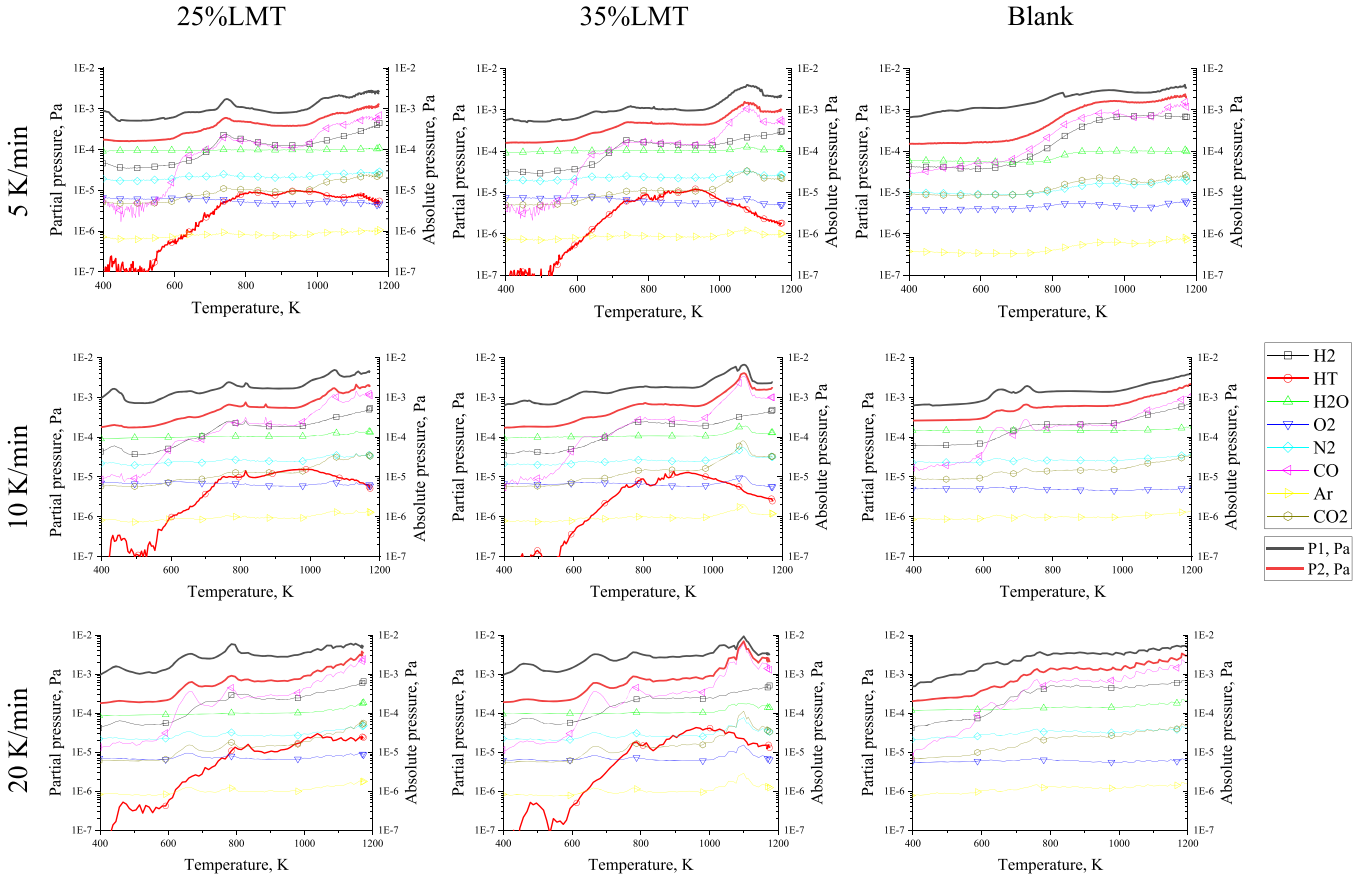

Fig. 4. TDS-experiment data: temperature dependence of the change in partial pressure of gas species for all samples and “blank” using different heating rates (β) in the range from 400 K to 1173 K.

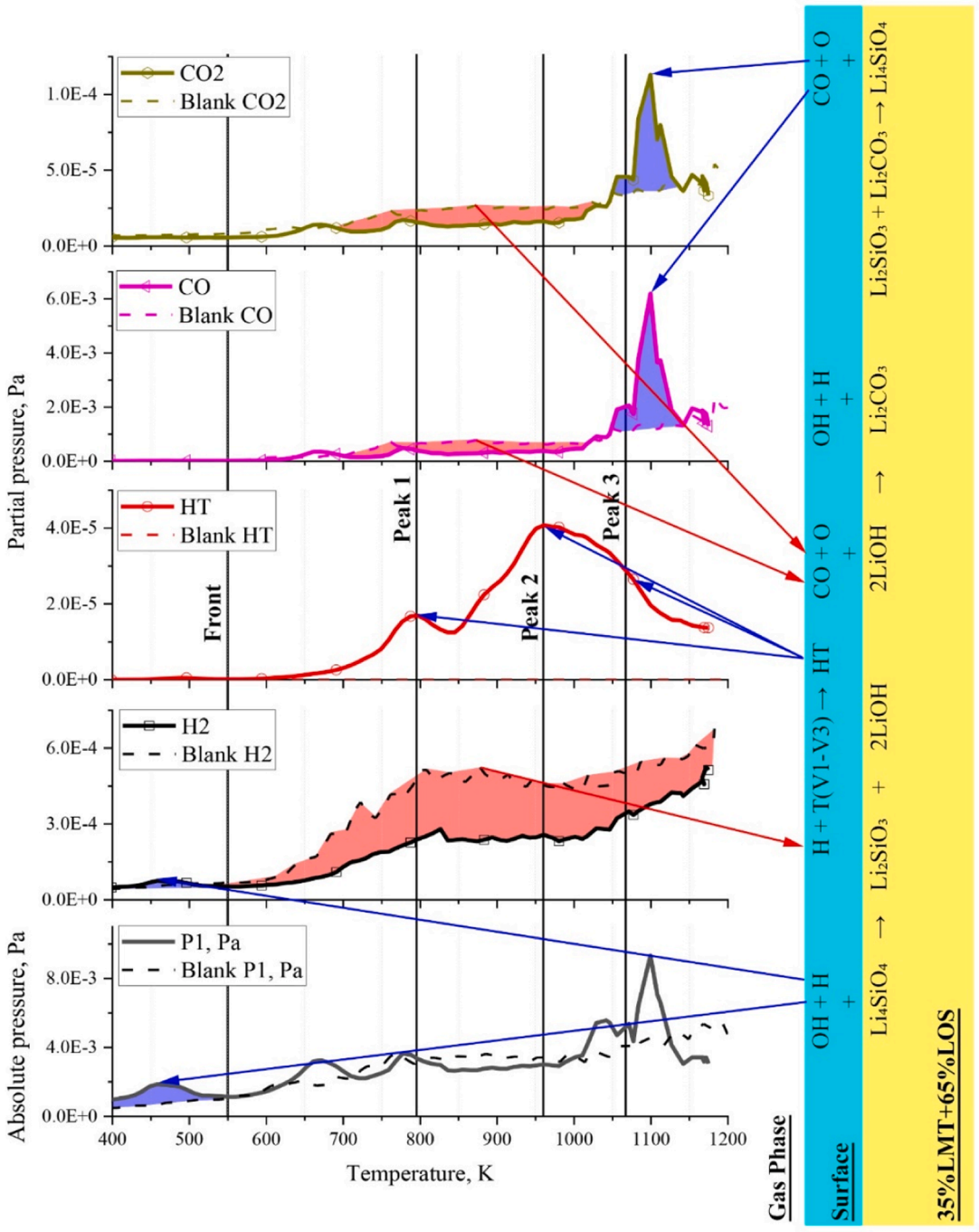

Fig. 5. Schematic representation of the main processes in ED with a sample of irradiated biphasic lithium ceramics using the example of the experiment with pebble No.6.

H_2 is especially noticeable, why tritium is released in the form of HT molecules under these conditions, and not being involved in reactions with the formation of other compounds. This seems to be due to the presence of significant amounts of H_2O, which form OH complexes and free H atoms on the sample surface. These hydrogen atoms actively react with tritium T to form HT molecules. In parallel, OH complexes interact back with hydrogen atoms H, leading to the formation of water H_2O. Also, the collision of hydrogen atoms leads to the formation of molecular hydrogen H_2.

Regarding the measurement results for different phase compositions of the samples, especially for batches with 35 %LMT, a peak release of the carbon-containing gases CO and CO_2 is observed. The process starts at about 1000 K and reaches a maximum around 1100 K. With increasing temperature, tritium atoms begin to block the near-surface layer of the sample, which slows down the processes of interaction of various components inside the material. At the same time, the reactions indicated in the chemical reactions (1) and (2) actively take place on the sample surface, which promotes the accumulation of carbonates. As a result, with a decreasing amount of released tritium, the pressure of CO and CO_2 begins to increase due to the delayed reactions (3). As can be seen from the graphs in Fig. 4, for samples with 25 %LMT the tritium release is more stable, which makes this reaction channels less active, as a consequence CO and CO_2 peaks are less pronounced. Schematic illustration of the main processes in ED with a sample of irradiated biphasic lithium ceramics on the example of the results of experiment No.6 (35 %LMT - 20 K/min) in comparison with the corresponding

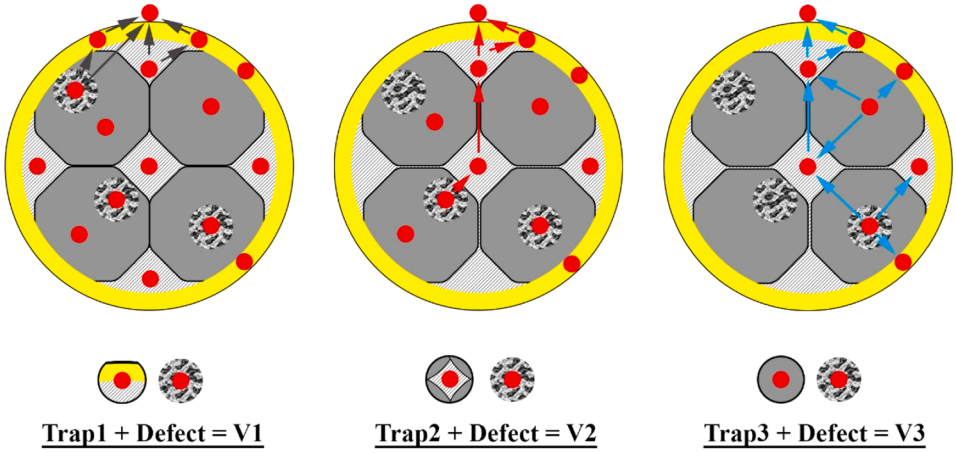

Fig. 6. Schematic illustration of the three main types of traps and associated defects in the structure of lithium ceramics.

blank experiment No.9 is shown in Fig. 5.

Hydration and transformation of lithium orthosilicate:

$$Li_4SiO_4 + H_2O\ (\text{on the surface}: OH + H) \rightarrow Li_2SiO_3 + 2LiOH \quad (1)$$

Interaction of lithium hydroxide with carbon dioxide to form carbonate:

$$2LiOH + CO_2(\text{on the surface}: \text{CO} + \text{O}) \rightarrow Li_2CO_3 + H_2O \quad (2)$$

Cyclic recovery of lithium orthosilicate:

$$Li_2SiO_3 + Li_2CO_3 \rightarrow Li_4SiO_4 + \text{CO}_2 \quad (3)$$

In the context of chemical reaction (3), CO is the main recovery product. The formation of CO_2 has also been observed, which may occur when the formation of CO reacts with excess oxygen. In addition, the excess oxygen atoms can be reduced to O_2, which is confirmed by the mass spectrum data.

Fig. 6 illustrates the three main types of traps and associated defects in the structure of biphasic lithium ceramics that play a key role in tritium release processes. This scheme helps to visualize the routes through which tritium can move in the material and highlights the importance of structural organization and trap characteristics for understanding the mechanisms of its release.

1. V1 – The sum of Trap1 and the defects leading to the surface: Trap1 contains tritium atoms located in open pores and near-surface layers of the material. These traps provide easier and more direct access of tritium to the outer surface, which facilitates its faster and more efficient release. Defects of various origins included in this category also have access to the surface, which increases the overall rate of tritium desorption.
2. V2 –Sum of Trap2 and defects leading to closed pores: Trap2 includes tritium atoms trapped in closed pores. These traps restrict the movement of tritium, making it difficult to escape because desorption requires additional energy to move tritium from deep within the material along the boundaries of the two grains to the surface or to other regions with less confinement.
3. V3 –The sum of Trap3 and various closed defects: Trap3 similarly to Trap2 contains tritium in closed pores, but in this case the emphasis is on even more closed and isolated structures inside the grains. Here, the tritium is even more isolated, which significantly slows its release and makes it dependent on complex diffusion processes and possible changes in the structural integrity of the material due to heating.

4.1. Characterization and weighing of samples after TDS

After TDS, all samples retained their geometric integrity and lost most of their black color (see Fig. 7), because the temperature effect promoted the recovery of oxygen atoms in the near-surface layer. The results of weighing after TDS showed no noticeable mass loss, remaining within the acceptable errors.

5. Analysis of results

Based on the partial pressures of HT gas in the mass spectrometer chamber, a calculated determination of the total amount of tritium in the working volume of the unit was made (see Fig. 8). The following key parameters were used to analyze the time dependence of changes in the number of tritium atoms in the entire working chamber:

1. *Volume of the working chamber:* the total volume of the working chamber was calculated, which amounted to about 7.2 Ls.
2. *Absolute pressure in the unit chamber (based on P1 and P2 data):* using numerical methods, the average pressure over the unit was determined, as there is a non-uniform distribution along the working path, where the pressure is minimum near the pumping area and maximum in the sample location area.

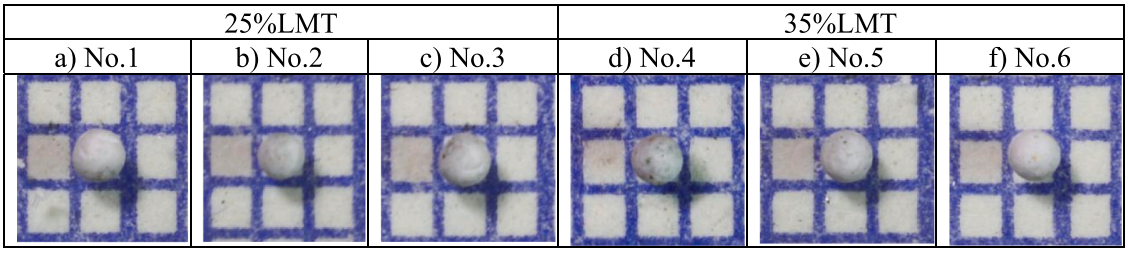

Fig. 7. Appearance of samples after TDS experiments.

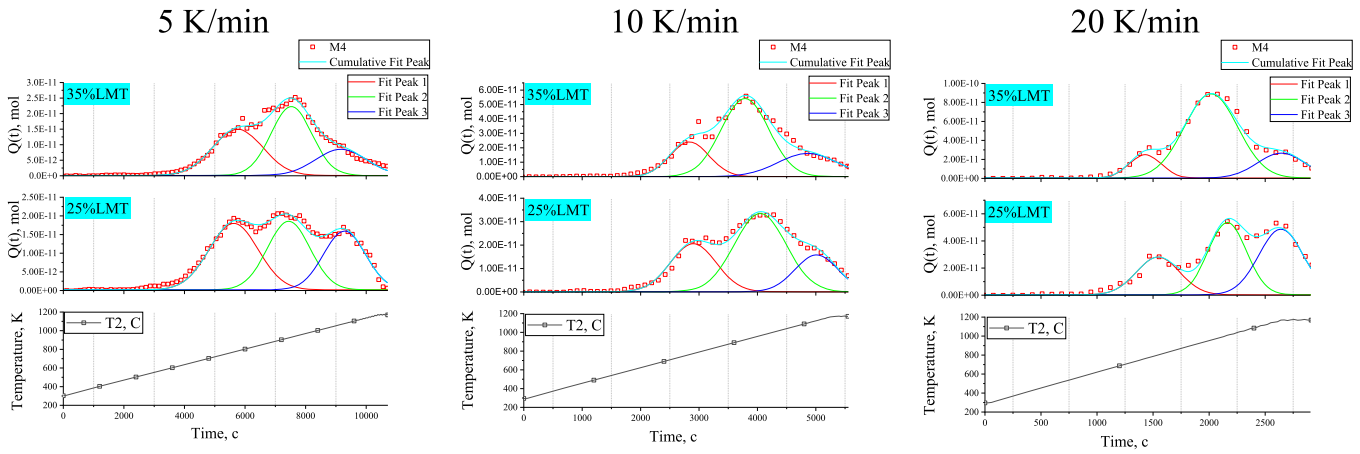

Fig. 8. Time dependence of change in the amount of tritium in the working chamber of the unit.

Table 4
Total amount of released tritium for the whole period of experiments No.1–6.

Heating rate, K/min	25 %LMT		35 %LMT	
	Q(t), mol	Q(t)/m, mol/mg	Q(t), mol	Q(t)/m, mol/mg
5	9.92E-08	6.75E-08	8.80E-08	6.77E-08
10	7.28E-08	6.22E-08	9.66E-08	8.40E-08
20	6.28E-08	4.94E-08	7.91E-08	6.59E-08

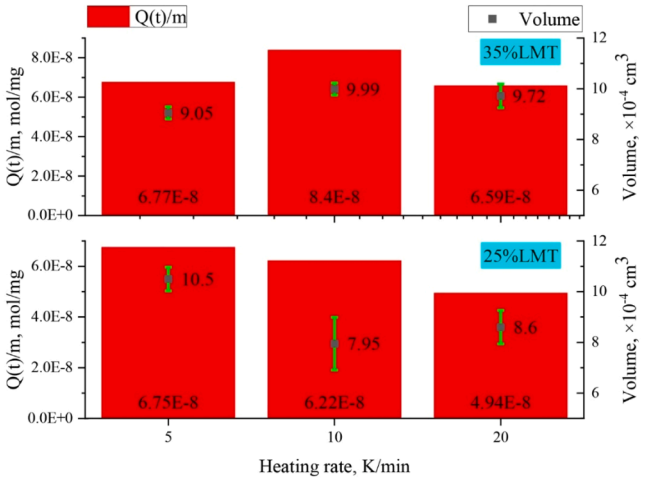

Fig. 9. Summary diagram illustrating tritium release per unit mass and comparisons with volumes.

3. *Average chamber wall temperature* calculated on the basis of careful analysis of the temperature field along the working path.

It is important to note here that the Fit Peak illustration was used in Fig. 8 to demonstrate possible peak overlap, possibly resulting in the formation of additional (auxiliary) peaks. However, the data from this fitting were not used for analytical analysis.

It is observed that the tritium release front for all samples occurs at the same temperature of about 550 K. From the analysis of the time variation of the amount of tritium in the unit by integration, the total amount of tritium released over the entire period of the experiment, denoted as $Q(t)$, was determined. In addition, the specific amount of tritium released per unit mass, denoted as $Q(t)/m$, was estimated. These values allow an estimation of the efficiency of the tritium release process as a function of heating rate for different types of lithium ceramics.

Table 5
Amount of released tritium for each individual Peaks 1–3 of 25 %LMT samples No.1–3.

Heating rate, K/min	Peak 1		Peak 2		Peak 3	
	Q(t), mol	V1, %	Q(t), mol	V2, %	Q(t), mol	V3, %
5	3.47E-08	34	4.41E-08	43	2.36E-08	23
10	2.22E-08	31	3.61E-08	50	1.33E-08	19
20	1.34E-08	23	2.76E-08	47	1.80E-08	31

Table 6
Amount of released tritium for each individual Peaks 1–3 of 35 %LMT samples No.4–6.

Heating rate, K/min	Peak 1		Peak 2		Peak 3	
	Q(t), mol	V1, %	Q(t), mol	V2, %	Q(t), mol	V3, %
5	2.65E-08	30	4.60E-08	53	1.48E-08	17
10	2.19E-08	23	5.28E-08	55	2.09E-08	22
20	1.25E-08	17	5.11E-08	68	1.19E-08	16

Table 4 summarises data for two types of lithium ceramics (25 %LMT and 35 %LMT) at different heating rates (5, 10, 20 K/min).

Overall, the experimental data are in good agreement with each other and are within the order of magnitude expected from tritium release calculations (see Table 1). Some differences may be related to the shape and morphology of the surface of the samples, which affects the total surface area of the samples, and the amount of tritium released. For clarity, a summary diagram comparing the values of $Q(t)/m$ with the volume of the samples is presented in Fig. 9, taking into account the calculation error due to the non-sphericity of the samples.

Comparison of theoretical calculations with experimentally determined values of the total amount of released tritium demonstrates a good agreement within the order of magnitude. This confirms that the used models and calculation methods adequately describe the processes of tritium release under the conditions of the experiments.

The analysis of the dynamics of tritium release from biphasic samples shows that the process is characterized by the presence of three peaks, showing different shifts depending on the heating temperature. These data are reflected in the Table 5 and Table 6, which show the changes in

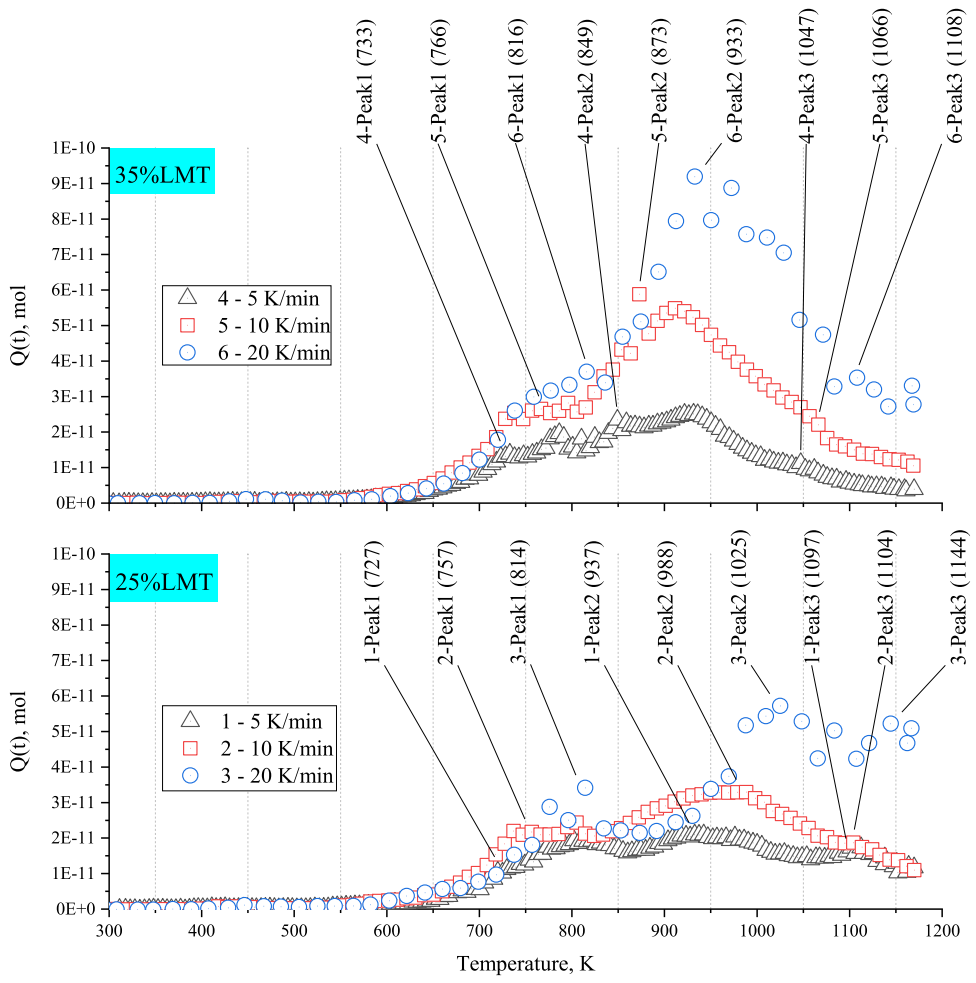

Fig. 10. Temperature dependence of tritium release for all samples No.1–6.

the amount of tritium released and its percentage of the total amount at different heating rates.

At higher heating rates, the peaks become more "blurred" and shift toward higher temperatures, which may be due to changes in the thermal desorption kinetics or changes in the mechanisms of tritium release.

Percentage analysis shows that as the heating rate increases, the fraction of tritium released at Peak 2 increases (see Table 5 and Table 6). This emphasizes the influence of heat treatment dynamics on the process of tritium release from the material.

By considering the different phases in biphasic lithium ceramic samples, it can be observed that the change in phase composition has a significant effect on the kinetics and dynamics of tritium release. From Table 5 and Table 6, it can be seen that different phase compositions react differently to temperature modes. Samples with a higher content of 35 %LMT show a higher rate of tritium release at lower temperature peaks compared to samples with a higher content of the main phase (25 %LMT). In the sample with the higher LOS content, the percentage of tritium released remains more stable at different heating rates, which may indicate a more stable structure or more efficient "traps" for tritium. With increasing heating rate, there is an increase in the amount of tritium released at Peak 2 due to the decrease in Peak 1 (see Table 5 and Table 6), which may be associated with more pronounced defects or reconfiguration of tritium "traps" in the material.

The 35 %LMT samples show higher tritium values at Peak 2 at all heating rates, so that the majority of the generated tritium is released at relatively low temperatures.

A kinetic analysis method based on the Arrhenius equation was used to estimate the activation energy (*Ea*) and pre-exponent (*K*0), which are

Table 7
Summary table of tritium release peaks of 25 %LMT samples No.1–3.

Heating rate, K/min	Peak 1		Peak 2		Peak 3	
	T, K	Q(t), mol	T, K	Q(t), mol	T, K	Q(t), mol
5	727	1.85E-11	937	2.04E-11	1097	1.57E-11
10	757	2.26E-11	988	3.27E-11	1104	1.56E-11
20	814	3.15E-11	1025	5.51E-11	1144	5.07E-11

Table 8
Summary table of tritium release peaks of 35 %LMT samples No.4–6.

Heating rate, K/min	Peak 1		Peak 2		Peak 3	
	T, K	Q(t), mol	T, K	Q(t), mol	T, K	Q(t), mol
5	733	1.64E-11	849	2.41E-11	1047	9.60E-11
10	766	2.64E-11	873	5.27E-11	1066	2.51E-11
20	816	3.69E-11	933	8.54E-11	1108	5.20E-11

written as follows in general representation:

$$K = K0 \cdot e^{-Ea/RT} \tag{4}$$

where R — universal gas constant (kJ/mol).

In this approach, the peaks of the TDS spectrum of tritium at different heating rates were analyzed. A summary diagram of tritium release versus temperature for different heating rates is given in Fig. 10. Here,

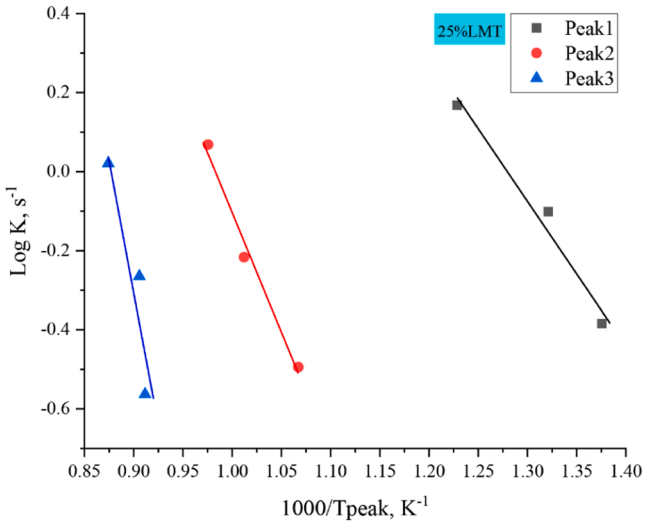

Fig. 11. Dependence **log*K*** from **1000/*Tpeak*** for samples 25 %LMT No.1–3.

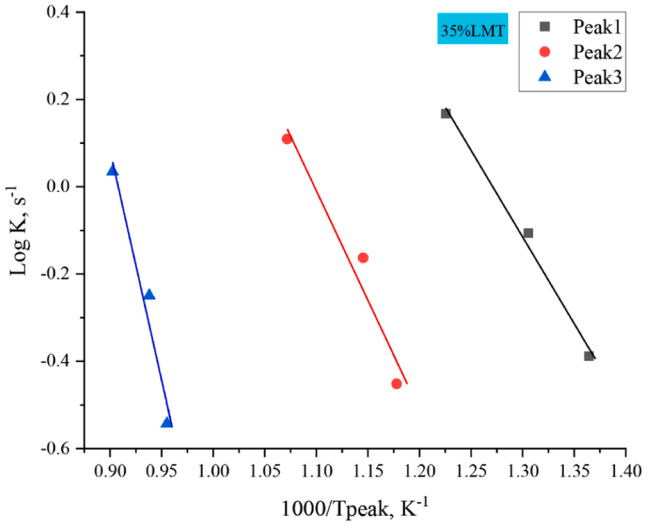

Fig. 12. Dependence **log*K*** from **1000/*Tpeak*** for samples 35 %LMT No.4–6.

Table 9
Kinetic parameters for samples with different phase ratios.

Batch	Peak 1	Peak 2	Peak 3
	25 %LMT		
*K*0, s^{-1}	$(49.9 \pm 5) \times 10^{3}$	$(90.0 \pm 9) \times 10^{4}$	$(54.3 \pm 5) \times 10^{10}$
Ea, kJ/mol	70 ± 3	116 ± 6	257 ± 13
Batch	35 %LMT		
*K*0, s^{-1}	$(11.1 \pm 1) \times 10^{4}$	$(32.3 \pm 3) \times 10^{4}$	$(36.0 \pm 4) \times 10^{8}$
Ea, kJ/mol	76 ± 3	96 ± 5	202 ± 10

the main peaks 1–3 of the selection were taken and the auxiliary peaks of the overlap were not analyzed. In Tables 7 and 8 data of the analyzed peaks 1–3 for two batches of samples are summarized.

Next, the determination of the parameters of the rate constant of peak separation was conducted:

$$\frac{\beta}{Tpeak} = K = \frac{dQ(t)}{dt}\cdot\frac{1}{Q(t)} \tag{5}$$

Due to Eq. (5) $\log K(s^{-1}) = log\ (\beta\,/Tpeak)$, where *Tpeak* (K) is the desorption peak temperature, and β (K/s) is the heating rate, the dependence $\log(\beta/Tpeak)$ from $1000/Tpeak$ was plotted for each experiment. The slope of this dependence allows the calculation of the activation energy and pre-exponents. These parameters were obtained for each temperature peak, which allows the description of the kinetics of tritium release during desorption (see Fig. 11 and 12).

The results of calculations of kinetic parameters for samples with different phase ratios of 25 %LMT and 35 %LMT show significant changes in the *K*0 and *Ea*, which is related not only to the phase composition but also to the change in the desorption mechanism (see Table 9). In the case of samples with 25 %LMT, relatively high values of *Ea* (70 257 kJ/mol) are observed, which may indicate complex diffusion pathways or the presence of more stable traps for tritium, requiring significant energy costs for its release. At the same time, when the LMT phase fraction is increased to 35 %, a decrease in *Ea* and a higher *K*0 value at peak 1 (see Table 9). This indicates faster desorption processes, probably related to changes in the microstructure or the number of active defects that facilitate tritium release at lower temperatures. Therefore, the results emphasize not only the phase dependence but also the role of microstructural features in changing the desorption and diffusion mechanisms.

To compare the obtained data with literature data, the values were recalculated in units of electron volts (eV), which is presented in Table 10. The results presented in this table emphasize the uniqueness of the present experiments and also demonstrate consistent trends based on comparative analysis of the experimental data. It can be seen from the comparison that low temperature conditions result in significantly higher values for all three desorption peaks compared to samples irradiated under high temperature conditions. This indicates deeper and more stable traps for tritium in the LT irradiated samples, leading to a more complex mechanism of tritium release despite the high neutron fluence.

6. Conclusion

TDS studies of biphasic lithium ceramic samples with different phase ratios of 25 %LMT and 35 %LMT after prolonged neutron irradiation (21.5 EFPD) have provided a deeper understanding of the principles of the tritium release process. The analysis allows the description of a reasonable mechanism of tritium release upon linear heating to 1173 K at different rates, which includes the following key points:

- Tritium release process: predominantly desorption with the release of tritium from the surface of the material in the form of HT molecules due to the presence of hydrogen in the system and on the surface of the sample.
- Effect of phase composition: the presence of a higher percentage of 35 %LMT in the samples shows enhanced tritium release, especially at lower temperatures, which emphasizes the importance of an optimal phase ratio to improve the performance of the ceramics.
- Tritium kinetics and distribution: tritium is uniformly distributed throughout the ceramic volume and its release is determined by the microstructural characteristics of the material, such as the presence and distribution of traps and defects.
- Integral and temperature aspects: evaluation of the integral quantities of extracted tritium shows a correlation of the calculation results between different samples, and the temperature dependence of the tritium desorption coefficient was clarified in further modeling.
- Final remarks: it was confirmed that different phase compositions of biphasic lithium ceramics affect the tritium release efficiency. The obtained results of the presented studies emphasize the importance of further investigation into biphasic lithium ceramics to assess their properties for tritium breeding in future fusion reactors such as DEMO.

Table 10
Comparison of values ***Ea*** obtained for Peaks 1–3 with the literature data.

Phase composition	Irradiation temperature	Fluence, n/cm^2	TDS method	Peak 1 *Ea*, eV	Peak 2 *Ea*, eV	Peak 3 *Ea*, eV
LOS [21]	high	7.9E15	Atmosphere (Ar)		0.29	
25 %LMT (this work)	low	3.7E19	Vacuum extraction	0.73	1.20	2.66
33 %LMT [19]	high	9.9E16	Atmosphere (Ar)	0.27	0.46	0.7
33 %LMT [20]	high	7.9E16	Atmosphere (Ar)		0.64	
35 %LMT (this work)	low	3.7E19	Vacuum extraction	0.79	1.01	2.09
50 %LMT [20]	high	7.9E16	Atmosphere (Ar)		0.76	
67 %LMT [19]	high	9.9E16	Atmosphere (Ar)	0.18	0.20	0.23
67 %LMT [20]	high	7.9E16	Atmosphere (Ar)		0.47	
LMT [19]	high	9.9E16	Atmosphere (Ar)	0.29	0.32	

Funding

The research has been funded by the Science Committee of the Ministry of Science and Higher Education of the Republic of Kazakhstan with Program No BR21881930.

CRediT authorship contribution statement

S. Askerbekov: Writing – original draft, Data curation, Conceptualization. **Y. Chikhray:** Supervision, Investigation, Formal analysis. **T. Kulsartov:** Methodology, Investigation, Formal analysis. **A. Akhanov:** Software, Methodology, Investigation. **A. Shaimerdenov:** Writing – review & editing, Supervision, Project administration. **M. Aitkulov:** Methodology, Investigation. **Zh. Bugybay:** Visualization, Project administration. **I. Kenzhina:** Validation, Project administration, Investigation. **Sh. Gizatulin:** Visualization, Validation, Resources, Methodology. **R. Knitter:** Writing – review & editing. **J. Leys:** Writing – review & editing.

Declaration of competing interest

The authors declare that they have no known competing financial interests or personal relationships that could have appeared to influence the work reported in this paper.

Data availability

The authors do not have permission to share data.

References

[1] R. Knitter, M.H.H. Kolb, U. Kaufmann, A.A. Goraieb, Fabrication of modified lithium orthosilicate pebbles by addition of titania, J. Nucl. Mater. 442 (2013) S433–S436, https://doi.org/10.1016/j.jnucmat.2012.10.034.

[2] M.H.H. Kolb, R. Knitter, T. Hoshino, Li4SiO4 based breeder ceramics with Li2TiO3, LiAlO2 and LiXLaYTiO3 additions, part II: pebble properties, Fusion Eng. Des. 115 (2017) 6–16, https://doi.org/10.1016/j.fusengdes.2016.12.038.

[3] G.J. Rao, R. Mazumder, S. Bhattacharyya, P. Chaudhuri, Fabrication and characterization of Li4SiO4-Li2TiO3 composite ceramic pebbles using extrusion and spherodization technique, J. Eur. Ceram. Soc. 38 (15) (2018) 5174–5183, https://doi.org/10.1016/j.jeurceramsoc.2018.07.018.

[4] C. Dang, M. Yang, Y.C. Gong, L. Feng, H.L. Wang, Y.L. Shi, Q.W. Shi, J.Q. Qi, T. C. Lu, A promising tritium breeding material: nanostructured 2Li2TiO3-Li4SiO4 biphasic ceramic pebbles, J. Nucl. Mater. 500 (2018) 265–269, https://doi.org/10.1016/j.jnucmat.2018.01.010.

[5] L.V. Boccaccini, F. Arbeiter, P. Arena, J. Aubert, L. Bühler, G. Zhou, Status of maturation of critical technologies and systems design: breeding blanket, Fusion Eng. Des 179 (2022), https://doi.org/10.1016/j.fusengdes.2022.113116. Article 113116.

[6] O. Leys, J.M. Leys, R. Knitter, Current status and future perspectives of EU ceramic breeder development, Fusion Eng. Des. 164 (2020), https://doi.org/10.1016/j.fusengdes.2020.112171.

[7] T. Kulsartov, Z. Zaurbekova, R. Knitter, A. Shaimerdenov, Y. Chikhray, S. Askerbekov, A. Akhanov, I. Kenzhina, G. Kizane, Y. Kenzhin, M. Aitkulov, D. Sairanbayev, Studies of two-phase lithium ceramics Li4SiO4-Li2TiO3 under conditions of neutron irradiation, Nucl. Mater. Energ. 30 (2022) 101129, https://doi.org/10.1016/j.nme.2022.101129.

[8] T. Kulsartov, Zh. Zaurbekova, R. Knitter, Ye. Chikhray, I. Kenzhina, S. Askerbekov, A. Shaimerdenov, G. Kizane, Reactor experiments on irradiation of two-phase lithium ceramics Li2TiO3/Li4SiO4 of various ratios, Fus. Eng. Des. 197 (2023) 114035, https://doi.org/10.1016/j.fusengdes.2023.114035.

[9] I. Kenzhina, T. Kulsartov, Y. Chikhray, Y. Kenzhin, Z. Zaurbekova, A. Shaimerdenov, G. Kizane, A. Zarins, A. Kozlovskiy, M. Gabdullin, A. Tolenova, Analysis of the reactor experiments results on the study of gas evolution from two-phase Li2TiO3-Li4SiO4 lithium ceramics, Nucl. Mater. Energ. 30 (2022) 101132, https://doi.org/10.1016/j.nme.2022.101132.

[10] M. Yang, L. Zhao, Y. Qin, G. Ran, Y. Gong, H. Wang, C. Xiao, X. Chen, T. Lu, Tritium release property of Li2TiO3-Li4SiO4 biphasic ceramics, J. Nucl. Mater. 538 (2020) 152268, https://doi.org/10.1016/j.jnucmat.2020.152268.

[11] M. Yang, L. Zhao, G. Ran, Y. Gong, H. Wang, S. Peng, C. Xiao, X. Chen, T. Lu, Tritium release behavior of Li2TiO3 and 2Li2TiO3-Li4SiO4 biphasic ceramic pebbles fabricated by microwave sintering, Fus. Eng. Des. 168 (2021) 112390, https://doi.org/10.1016/j.fusengdes.2021.112390.

[12] Q. Zhou, F. Sun, S. Hirata, S. Li, Y. Li, Y. Oya, Effect of neutron dose on the tritium release behavior of Li2TiO3–0.5Li4SiO4 biphasic ceramic, Int. J. Hydrog. Energy 48 (2023) 4363–4370, https://doi.org/10.1016/j.ijhydene.2022.11.009.

[13] Q. Zhou, S. Li, S. Hirata, A. Sanfukuji, G. Tan, A. Taguchi, Y. Oya, Tritium and deuterium release behavior of Li2TiO3-0.5Li4SiO4–Pb ceramic, Ceram. Int. 49 (16,15) (2023) 26778–26785, https://doi.org/10.1016/j.ceramint.2023.05.214.

[14] Q. Qi, J. Wang, Q. Zhou, Y. Zhang, M. Zhao, S. Gu, G.-N. Luo, Comparison of tritium release behavior in Li2TiO3 and promising core-shell Li2TiO3–Li4SiO4 biphasic ceramic pebbles, J. Nucl. Mater. (2020) 152330, https://doi.org/10.1016/j.jnucmat.2020.152330.

[15] J.M. Heuser, M.H.H. Kolb, T. Bergfeldt, R. Knitter, Long-term thermal stability of two-phased lithium orthosilicate/metatitanate ceramics, J. Nucl. Mater. 507 (2018) 396–402, https://doi.org/10.1016/j.jnucmat.2018.05.010.

[16] A. Shaimerdenov, S. Gizatulin, D. Dyussambayev, S. Askerbekov, I. Kenzhina, The WWR-K reactor experimental base for studies of the tritium release from materials under irradiation, Fusion Sci. Technol. 76 (3) (2020) 304–313, https://doi.org/10.1080/15361055.2020.1711852.

[17] J. Leys, R. Rolli, H.-C. Schneider, R. Knitter, HICU PIE results of neutron-irradiated lithium metatitanate pebbles, Nucl. Mater. Energy 38 (2024) 101625, https://doi.org/10.1016/j.nme.2024.101625.

[18] Y. Chikhray, S. Askerbekov, R. Knitter, T. Kulsartov, A. Shaimerdenov, M. Aitkulov, A. Akhanov, D. Sairanbayev, Z. Bugybay, A. Nessipbay, K. Kisselyov, G. Kizane, A. Zarins, Studies of irradiated two-phase lithium ceramics Li4SiO4/Li2TiO3 by thermal desorption spectroscopy, Nucl. Mater. Energy 38 (2024) 101621, https://doi.org/10.1016/j.nme.2024.101621.

[19] Q. Qi, M. Zhao, F. Sun, Y. Zhang, S. Gu, B. Ji, H.-S. Zhou, Y. Oya, S. Liu, G.-N. Luo, Investigation on effects of tritium release behavior in Li4SiO4 pebbles, Nucl. Mater. Energy 28 (2021) 101036, https://doi.org/10.1016/j.nme.2021.101036.

[20] Q. Zhou, A. Togari, M. Nakata, M. Zhao, F. Sun, Q. Xu, Y. Oya, Release kinetics of tritium generation in neutron irradiated biphasic Li2TiO3-Li4SiO4 ceramic breeder, J. Nucl. Mater. 522 (2019) 286–293, https://doi.org/10.1016/j.jnucmat.2019.05.033.

[21] S. Hirata, K. Ashizawa, F. Sun, Y. Feng, X. Wang, H. Wang, M. Kobayashi, A. Taguchi, Y. Oya, Tritium recovery behavior for tritium breeder Li4SiO4-Li2TiO3 biphasic material, J. Nucl. Mater. 567 (2022) 153838, https://doi.org/10.1016/j.jnucmat.2021.153838.